

RESEARCH

Open Access



Mechanism of lncRNA ZFAS1 mediating nucleus pulposus cell pyroptosis in intervertebral disc degeneration

Yuchun Fu^{1*}, Leilei Zhu² and Bingxu Ma³

Abstract

Background This study investigates the mechanism of lncRNA ZFAS1 in pyroptosis of TNF- α -induced nucleus pulposus cells (NPCs) in intervertebral disc degeneration (IDD).

Methods Mouse NPCs were isolated and induced by TNF- α to establish a cell model of IDD. The cell viability was evaluated by MTT assay. NLRP3, GSDMD-N, and cleaved-Caspase1 expressions were detected by Western blot. IL-1 β and IL-18 contents were detected by ELISA. RT-qPCR was performed to determine ZFAS1, miR-155-3p, and METTL14 expressions. After intervening in ZFAS1 expression, the effect of ZFAS1 on pyroptosis was verified by Western blot and ELISA assays. RNA pull down or dual luciferase assay verified the binding between ZFAS1, miR-155-3p, and METTL14.

Results TNF- α induced pyroptosis of NPCs and promoted ZFAS1 expression. Silence of ZFAS1 repressed pyroptosis of TNF- α -induced NPCs. Mechanistically, ZFAS1 upregulated the transcription of METTL14 by competitively binding to miR-155-3p, thus enhancing NLRP3/Caspase-1-mediated NPC pyroptosis. Inhibition of miR-155-3p or overexpression of METTL14 alleviated the inhibitory effect of ZFAS1 silencing on TNF- α -treated NPC pyroptosis.

Conclusion ZFAS1 facilitates NLRP3/Caspase-1-mediated pyroptosis of NPCs in IDD via miR-155-3p/METTL14 axis.

Keywords Intervertebral disc degeneration, Nucleus pulposus cells, Pyroptosis, ZFAS1, miR-155-3p

Introduction

Intervertebral disc degeneration (IDD) underlies the primary contributor to low back pain (LBP) and even insults severe neurological complications, which not only significantly compromises the quality of life and work efficiency of patients but also poses a substantial socio-economic

burden worldwide [1]. Currently, the available treatments such as spinal fusion and anti-inflammatory medication can merely alleviate pain symptoms but fail to restore the disc structure and mechanical function [2]. At the cellular level, IDD can be partially attributed to the aberrant pathological alternations in the life process of nucleus pulposus cells (NPCs) in the intervertebral disc (IVD), including proliferation, senescence, apoptosis, inflammation, and extracellular matrix (ECM) remodeling [3]. Particularly, NPC death has been acknowledged as one of the initiating events of IDD, leading to loss of cellular function, reduced nutrient synthesis and repair ability, as well as enhanced inflammation, all of which exacerbate the degenerative cascade of IDD [4, 5]. Pyroptosis is a type of pro-inflammatory programmed cell death

*Correspondence:

Yuchun Fu

fuyuchun1997@163.com

¹Bengbu Medical University, 2600 Donghai Avenue, Bengbu, Anhui Province 233000, China

²Physical Examination Center of the First Affiliated Hospital of Bengbu Medical University, Bengbu 233004, China

³Department of Minimally Invasive Spine Surgery, Bengbu First People's Hospital, Bengbu 233000, China



© The Author(s) 2025. **Open Access** This article is licensed under a Creative Commons Attribution-NonCommercial-NoDerivatives 4.0 International License, which permits any non-commercial use, sharing, distribution and reproduction in any medium or format, as long as you give appropriate credit to the original author(s) and the source, provide a link to the Creative Commons licence, and indicate if you modified the licensed material. You do not have permission under this licence to share adapted material derived from this article or parts of it. The images or other third party material in this article are included in the article's Creative Commons licence, unless indicated otherwise in a credit line to the material. If material is not included in the article's Creative Commons licence and your intended use is not permitted by statutory regulation or exceeds the permitted use, you will need to obtain permission directly from the copyright holder. To view a copy of this licence, visit <http://creativecommons.org/licenses/by-nc-nd/4.0/>.

mediated by the activation of inflammasomes [6]. Emerging evidence has highlighted the critical implication of NLRP3 inflammasome-mediated pyroptosis of NPCs in the progression of IDD [7]. Hence, it is necessary to further clarify the mechanism of NPC pyroptosis to improve the clinical outcomes of IDD.

Long non-coding RNAs (lncRNAs) are a class of RNA transcripts >200 nucleotides with no protein-coding capacity and function as vital diagnostic indicators and therapeutic targets in the pathological progression of IDD [8, 9]. One of such lncRNAs, zinc finger antisense 1 (ZFAS1) is highly expressed in degenerative NP tissues and IL-1 β -induced NPCs [10]. Moreover, elevated ZFAS1 has been correlated with exacerbated disease severity and augmented inflammation in IDD patients [11]. However, whether lncRNA ZFAS1 promotes pyroptosis of NPCs remains unknown.

Mechanistically, lncRNAs function as competing endogenous RNAs (ceRNAs) by competitively binding to microRNAs (miRNAs), thus modulating the expressions of target mRNAs [12]. miRNAs, a family of evolutionarily conserved ncRNAs (~22 nucleotides in length), manipulate gene expression by binding to the 3'-untranslated region of target mRNAs [13]. There are complex interactions between miRNAs and target genes critical for the control of musculoskeletal conditions such as osteoarthritis [14], tendon injuries [15, 16], rheumatoid arthritis [17], and osteoporosis [18]. Particularly, a variety of miRNAs have been demonstrated to participate in the pathological processes of IDD by mediating NPC apoptosis, inflammatory responses, and ECM degradation [19]. ZFAS1 facilitates NPC apoptosis and ECM degradation via miR-4711-5p-dependent suppression of AKK1 [10]. Silence of ZFAS1 promotes proliferation but suppresses apoptosis of tumor necrosis factor- α (TNF- α)-treated synoviocytes by competitively binding to miR-296-5p [20]. We predicted a binding relationship between ZFAS1 and miR-155-3p through the RNA22 website. Reduced miR-155-3p expression is presented in degenerative NP tissues from IDD patients, and elevated miR-155-3p boosts the proliferation but represses the apoptosis of NPCs [21]. Moreover, elevation of miR-155 leads to a decrease in MMP-16 and an increase in aggrecan, thereby retarding IDD progression [22]. Based on the above findings, we speculate that lncRNA ZFAS1 acts as a miR-155-3p sponge to induce pyroptosis of NPCs in IDD. The specific mechanism of ZFAS1 promoting pyroptosis of NPCs revealed in this study may provide a new theoretical basis for the treatment of IDD.

Materials and methods

Ethics statement

All animal experiment schemes were approved by the Animal Ethics Committee of Bengbu Medical University

and implemented based on the *Guide for the Care and Use of Laboratory Animals* [23].

Cell culture

Three 3-month-old male C57BL/6 mice were purchased from Vital River Laboratory Animal Technology Co., Ltd (Shanghai, China) [SYXK (Shanghai) 2022-0018]. According to the methods described in previous literature, NPCs were isolated from the lumbar disc of mice [24]. In short, mice were euthanized with 3% pentobarbital sodium (150 mg/kg) and their lumbar vertebrae were isolated under sterile conditions. After separating the central NP tissue under a dissecting microscope, the IVD tissue was cut into 0.1 mm \times 0.1 mm pieces and incubated sequentially with 0.25% trypsin and 0.2% type I collagenase at 37 $^{\circ}$ C for 15 min. After filtering through a 70- μ m filter (542070, Greiner), the suspension was centrifuged at 300 g for 5 min. Then, the cell precipitation was transferred into a culture flask containing DMEM/F12 supplemented with 15% fetal bovine serum. About 5 days after separation, the spindle-shaped cells adhered to the bottom were the 0th generation NPCs. When 80–90% confluence was reached, NPCs were detached with 0.25% trypsin, followed by continue subculture. The 3rd generation NPCs were used in each experiment of this study.

Cell identification

NPCs were fixed with 4% paraformaldehyde for 0.5 h, cultured with 0.1% Triton X-100 for another 15 min, and then blocked with 2% bovine serum albumin (Sigma-Aldrich, Merck KGaA, Darmstadt, Germany) for another 1 h. Afterwards, NPCs were exposed to collagen II antibody (ab34712, Abcam, Cambridge, MA, USA) at 4 $^{\circ}$ C overnight and then to Alexa Fluor[®] 488-labeled secondary antibody (ab150077, Abcam). After washing with phosphate-buffered saline (PBS) three times, NPCs were stained with 4',6'-diamidino-2-phenylindole. The images were observed under a laser confocal microscope (OLYMPUS, Tokyo, Japan).

NPCs were subjected to trypsin treatment, and the cell concentration was adjusted to 1×10^9 cells/L. Two tubes were set up, with 1 mL of cells added to each tube (352235, Corning Falcon, NY, USA). One of the tubes was filled with 100 μ L of CD24-PE antibody (1:20, ab25494, Abcam), while another tube was added with isotype control (1:20, ab154450, Abcam). After 30 min of light avoidance treatment, the cells were added with 500 μ L of PBS containing 10 g/L paraformaldehyde and measured by a flow cytometer (Beckman Coulter, CA, USA). Negative cells were determined according to the fluorescence intensity of the isotype control, and the CD24-positive expression rate in NPCs was observed.

Cell treatment and transfection

The cells were treated with different doses of TNF- α (SRP2102; Sigma-Aldrich) at 37°C and 95% humidity in an atmosphere of 5% CO₂ for 24 h, with untreated cells as controls.

The cells were seeded into a 24-well culture dish (5×10^4 cells/well). When the cell confluence reached 70%, the cells were transfected with methyltransferase-like 14 (METTL14) overexpression vector (oe-METTL14) (50 nM), miR-155-3p inhibitor (inhi-155) (100 nM), si-ZFAS1 (50 nM), and corresponding negative controls of the same dose using Lipofectamine 3000 (Invitrogen, CA, USA). All sequences were purchased from Gene-Seed Biotechnology Co., Ltd (Guangzhou, China).

3-(4,5-dimethylthiazol-2-yl)-2,5-diphenyltetrazolium bromide (MTT) assay

The cells were detached with 0.25% trypsin and prepared into single cell suspension (5×10^3 cells/mL). The cells were seeded into a 96-well plate (100 μ L/well), incubated with 5 μ g/mL MTT solution (Sigma-Aldrich) (20 μ L/well), and then added with dimethyl sulfoxide (Sigma-Aldrich) (200 μ L/well). The optical density (OD490) was measured by a microplate reader (BioRad, California, USA).

Enzyme-linked immunosorbent assay (ELISA)

The cells were cultured at 37°C 5×10^4 cells/well). The levels of IL-1 β (ab197742, Abcam) and IL-18 (ab216165, Abcam) in cell culture supernatant (centrifugation 500 g, 4°C for 5 min) using ELISA kits. The optical density of each well was measured by Multiskan™ spectral spectrophotometer (Thermo Fisher Scientific, Waltham, MA, USA).

Nuclear and cytoplasmic fractionation assay

The subcellular localization of lncRNA ZFAS1 was predicted through the lncAtlas website (https://lncatlas.crg.eu/?tdsourcetag=s_pcqq_aiomsg) [25]. The nuclear/cytoplasmic extract was prepared using NE-PER nuclear and cytoplasmic extraction kit (Thermo Fisher Scientific). After 15 s of vortex oscillation, the cell precipitates were suspended in 1 mL of cytosol extraction reagent (CER) I (10 times the volume of the cell precipitation) containing phenylmethylsulfonyl fluoride (PMSF). Then, the suspension was incubated on ice for 10 min, added with CER II (CERI: CERII: nuclear extraction reagent (NER)=20:11:100), and vortexed for 5 s, followed by incubation on ice for 1 min and centrifugation at 16,000 g for 5 min. The supernatant (cytoplasmic extract) was transferred into the pre-cooled tube. The insoluble precipitate containing coarse nuclei was subjected to vortex oscillation for 15 s, resuspended in 1 mL of NER with PMSF (PMSF: NER=1:100), and incubated on ice for

40 min. The supernatant after centrifugation (16000 g, 10 min) was the nuclear extract. Reverse transcription quantitative polymerase chain reaction (RT-qPCR) was performed to detect the expression of ZFAS1 in nuclear and cytoplasmic extracts, with glyceraldehyde-3-phosphate dehydrogenase (GAPDH) and U6 as controls.

RNA pull down

The biotinylated-ZFAS1 (Bio-ZFAS1), ZFAS1 MUT (Bio-ZFAS1-MUT), miR-155-3p (Bio-miR-155-3p), miR-155-3p MUT (Bio-miR-155-3p-MUT), and NC (Bio-NC or Bio-miR-NC) were transfected into cells. The cell lysis buffer was incubated with dynabead M-280 Streptavidin (Invitrogen, Carlsbad, CA, USA) on ice for 10 min, followed by RT-qPCR. The biotinylated RNA was obtained for Sangon Biotech Co. Ltd (Shanghai, China).

Dual-luciferase assay

The binding site between lncRNA ZFAS1 and miR-155-3p was predicted through the RNA22 website (<http://cm.jefferson.edu/rna22/Interactive/>) [26]. The binding site between miR-155-3p and METTL14 was predicted through the TargetScan website (https://www.targetscan.org/vert_71/) [27]. The wild-type (WT) and mutant-type (MUT) pmirGLO ZFAS1/METTL14 were purchased from GenScript Co, Ltd (Nanjing, China). ZFAS1/METTL14-WT/MUT and miR-155-3p mimics (GenePharma, Shanghai, China) were co-transfected into logarithmic-grown cells at 70% confluence. The luciferase activity was determined using luciferase assay kit (Biovision, San Francisco, CA, USA) and Glomax20/20 spectrophotometer (Promega, Madison, WI, USA).

Real-time reverse transcriptase-polymerase chain reaction (RT-qPCR)

To evaluate the mRNA expressions of lncRNA ZFAS1, miR-155-3p, and METTL14, the total RNA was extracted using TRIzol reagent (Invitrogen). The DN-1000 Nanodrop spectrophotometer (Thermo Fisher Scientific) was used to assess the RNA concentration and purity. The total RNA was reverse transcribed into cDNA using reverse transcription kit (TOYOBO, Osaka, Japan). Real-time PCR was performed on the Stratagene MAXP3000 PCR System with SYBR FAST Master mix kit (KAPA, Boston, MA, USA). The relative expression of genes was calculated by the $2^{-\Delta\Delta C_t}$ method [28], with GAPDH and U6 as the internal references [21]. The primers are shown in Table 1.

Western blot

The total protein was extracted from cells using radio-immunoprecipitation assay (Thermo Fisher Scientific), and the total protein concentration of each sample was evaluated using bicinchoninic acid assay kit (Price

Table 1 PCR primer sequences

Name	Sequence (5'-3')
LncRNA ZFAS1	F: CGGCTCGGGGACTACATTTTC R: AACGAAAGGACGAGAGCGG
miR-155-3p	F: GGCCTCCTCTACCTGTTAG R: TGTCGTGGAGTCGGCAATTC
METTL14	F: GCACAGACGGGGACTTCATT R: TCCCAAAGAGATGAAGGCGT
U6	F: CGCTTCGGCAGCACATATACT R: CTTCACGAATTTGCGTGTCAT
GAPDH	F: GGTCCCAGCTTAGGTTTCATCA R: AATCCGTTACACCGACCTT

Note LncRNA ZFAS1: Long noncoding RNA zinc finger antisense 1; miR-155-3p: microRNA-155-3p; METTL14: methyltransferase-like 14; GAPDH: glyceraldehyde-3-phosphate dehydrogenase

Biotechnology, Rockford, IL, USA). Then, 20 µg of total protein was transferred onto polyvinylidene fluoride membranes (Millipore, MA, USA). The membranes were blocked with 5% skim milk and incubation with the primary antibodies at 4°C overnight, followed by incubation with the secondary antibody (ab205718, 1:2000, Abcam) for 1 h. The enhanced chemiluminescence kit (Millipore) was used to visualize the bands. The density of western blot results was detected using Image J Software. The ratio of target protein density to β-actin density was calculated to evaluate protein expression. The used primary antibodies were METTL14 (ab309096, 1:1000, Abcam), NLRP3 (ab263899, 1:1000, Abcam), GSDMD-N (A18281, 1:1000, Abclonal), cleaved-Caspase1 (PA5-38099, 1:1000, Thermo Fisher Scientific), and β-actin (ab5694, 1:1000, Abcam).

Statistical analysis

Data analysis and map plotting were performed using the SPSS 21.0 (IBM Corp., Armonk, NY, USA) and GraphPad Prism 8.0 (GraphPad Software Inc., San Diego, CA, USA). The data were examined for normal distribution and homogeneity of variance. The t test was adopted for comparisons between two groups, and one-way or two-way analysis of variance (ANOVA) was employed for the comparisons among multiple groups, following Tukey's multiple comparison test. A value of $P < 0.05$ indicated a significant difference.

Results

ZFAS1 is highly expressed in TNF-α-treated NPCs and promotes pyroptosis

ZFAS1 can accelerate the progression of IDD [10, 11], but its role in NPC pyroptosis in IDD is still unclear. We isolated NPCs and cultured them in vitro. Immunofluorescence staining of NPCs showed positive, indicating enrichment of type II collagen in NPCs (Fig. 1A). Flow cytometry results demonstrated CD24-positive in NPCs (Fig. 1B). Next, we induced NPCs with different

concentrations of TNF-α and found that as the concentration increased, the cell viability was gradually abated and ZFAS1 expression was elevated ($P < 0.01$, Fig. 1C-D). Based on the above results, we chose 30 ng/mL of TNF-α for subsequent experimentation. We reduced ZFAS1 expression in cells by transfecting siRNA ($P < 0.01$, Fig. 1D), followed by TNF-α treatment. The cell activity inhibited by TNF-α was enhanced after silence of ZFAS1 ($P < 0.01$, Fig. 1C). After treatment with TNF-α, the expressions of pyroptosis-related proteins (NLRP3, GSDMD-N, and cleaved-Caspase1) were notably increased, while silence of ZFAS1 diminished these proteins ($P < 0.01$, Fig. 1E). In addition, TNF-α induction upregulated pyroptosis-related factors IL-1 β and IL-18, while silence of ZFAS1 led to the opposite trends ($P < 0.01$, Fig. 1F). The above results indicate that ZFAS1 is highly expressed in TNF-α-treated NPCs and promotes pyroptosis.

ZFAS1 targets miR-155-3p expression

We predicted the subcellular localization of ZFAS1 and found that it was mainly located in the cytoplasm (Fig. 2A). Subsequent nuclear and cytoplasmic fractionation assay also confirmed the cytoplasmic localization of ZFAS1 (Fig. 2B), suggesting that ZFAS1 can regulate the expression of downstream genes through the ceRNA mechanism. miR-155-3p is downregulated in IDD [21]. The binding site between ZFAS1 and miR-155-3p was predicted through the RNA22 website (Fig. 2C). We speculated that miR-155-3p acted as a downstream miRNA of ZFAS1. RNA pull down assay verified the binding relationship between ZFAS1 and miR-155-3p ($P < 0.01$, Fig. 2D). Dual-luciferase assay further confirmed the target binding between ZFAS1 and miR-155-3p ($P < 0.01$, Fig. 2E). In addition, miR-155-3p expression was declined with the increase of TNF-α concentration but elevated with the decrease of ZFAS1 expression ($P < 0.01$, Fig. 2F). The above results indicate that ZFAS1 targets miR-155-3p expression.

Inhibition of miR-155-3p alleviates the inhibitory effect of ZFAS1 silencing on TNF-α-treated NPC pyroptosis

We inhibited miR-155-3p expression in TNF-α-treated NPCs for a combined treatment with si-ZFAS1*1 ($P < 0.01$, Fig. 3A-B). Inhibition of miR-155-3p weakened the cell viability ($P < 0.01$, Fig. 3C) and also elevated the expressions of NLRP3, GSDMD-N, and cleaved-Caspase1, as well as the levels of IL-1β and IL-18 ($P < 0.01$, Fig. 3D-E). These results suggest that inhibition of miR-155-3p alleviates the inhibitory effect of ZFAS1 silencing on TNF-α-treated NPC pyroptosis.

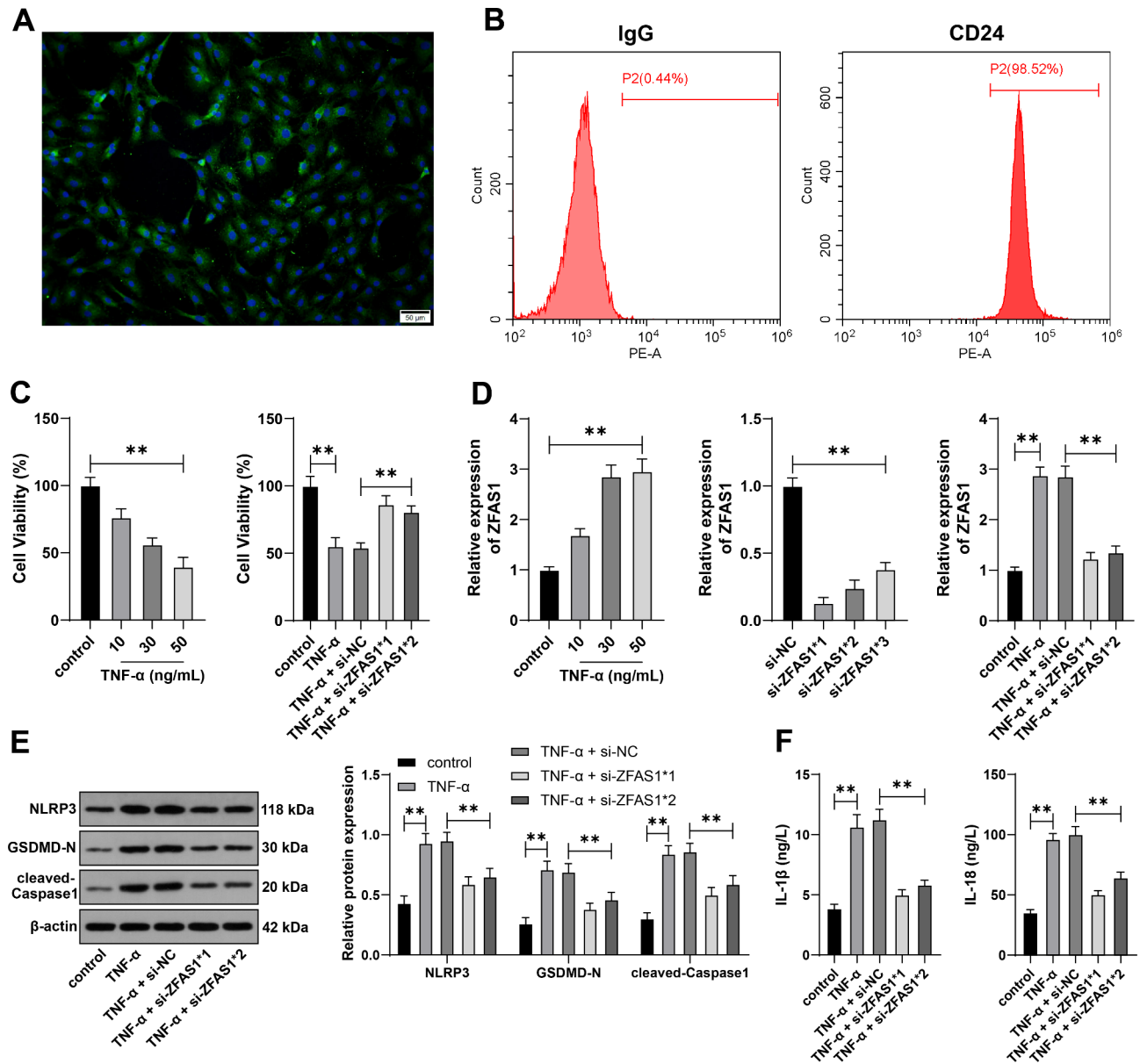


Fig. 1 ZFAS1 is highly expressed in TNF- α -treated NPCs and promotes pyroptosis. **A:** Mouse NPCs were identified using collagen II immunofluorescence staining. **B:** CD24 expression in mouse NPCs was determined using flow cytometry. **C:** Cell viability was assessed using MTT assay. **D:** ZFAS1 expression in cells was detected using RT-qPCR. **E:** NLRP3, GSDMD-N, and cleaved-Caspase1 expressions in cells were detected using western blot. **F:** IL-1 β and IL-18 levels were detected using ELISA. The cell experiments were repeated 3 times independently. The data are expressed as mean \pm standard deviation. The data in panels **C-D, F** were analyzed by one-way ANOVA, and the data in panel **E** were analyzed by two-way ANOVA, followed by Tukey's multiple comparisons test. ** $P < 0.01$

ZFAS1 facilitates METTL14 expression via the ceRNA mechanism

The binding relationship between miR-155-3p and METTL14 was predicted through the Targetscan database (Fig. 4A). METTL14 is highly expressed in IDD and promotes pyroptosis by stabilizing NLRP3 expression [29, 30]. Dual-luciferase assay further confirmed the target binding between METTL14 and miR-155-3p ($P < 0.01$, Fig. 4B). In addition, METTL14 expression was elevated with the increase of TNF- α concentration,

reduced with the decrease of ZFAS1 expression, and increased with the decrease of miR-155-3p expression ($P < 0.01$, Fig. 4C-D). The above results indicate that ZFAS1 promotes METTL14 expression by competitively binding to miR-155-3p.

Overexpression of METTL14 alleviates the inhibitory effect of ZFAS1 silencing on TNF- α -treated NPC pyroptosis

Finally, we overexpressed METTL14 expression in cells for a combined treatment with si-ZFAS1*1 ($P < 0.01$,

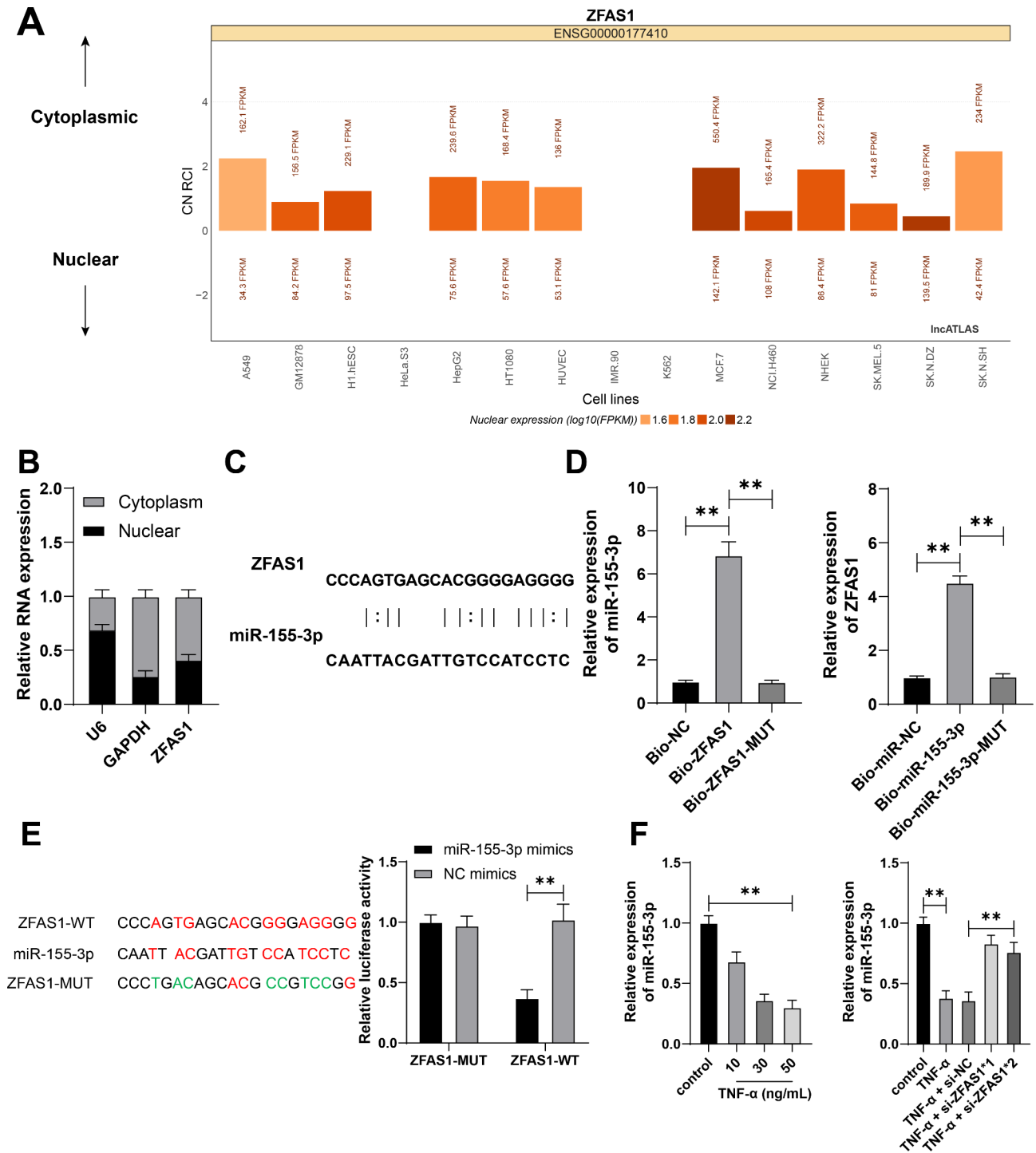


Fig. 2 ZFAS1 targets miR-155-3p and inhibits its expression. **A:** The subcellular localization of ZFAS1 was predicted through the IncAtlas website. **B:** The subcellular localization of ZFAS1 was detected using nuclear and cytoplasmic fractionation assay. **C:** The binding site between ZFAS1 and miR-155-3p was predicted through the RNA22 website. **D-E:** The binding relationship between ZFAS1 and miR-155-3p was validated using RNA pull down and dual-luciferase assay. **F:** miR-155-3p expression in cells was detected using RT-qPCR. The cell experiments were repeated 3 times independently. The data are expressed as mean \pm standard deviation. The data in panels **D, F** were analyzed by one-way ANOVA, and the data in panel **E** were analyzed by two-way ANOVA, followed by Tukey's multiple comparisons test. ****** $P < 0.01$

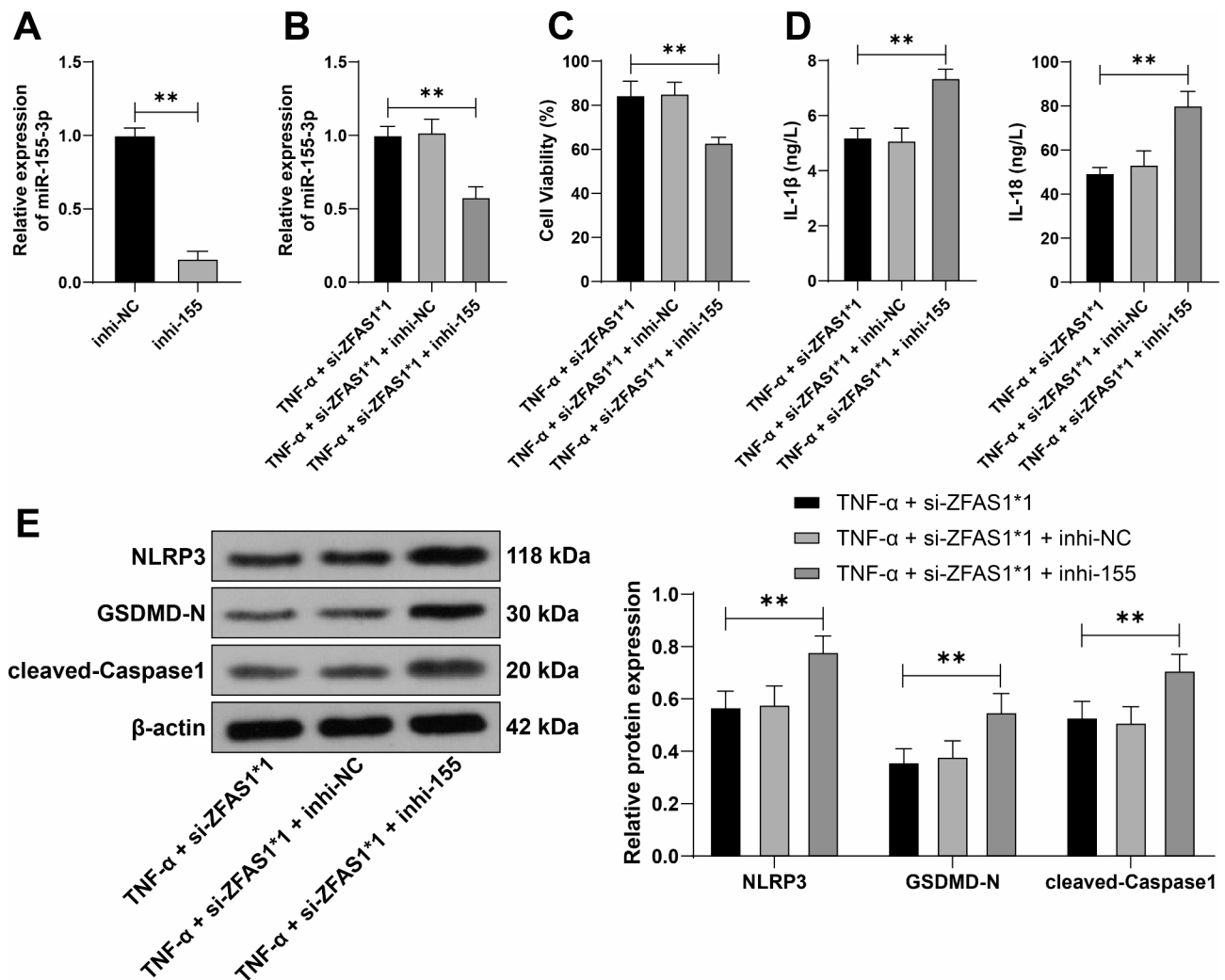


Fig. 3 Inhibition of miR-155-3p alleviates the inhibitory effect of ZFAS1 silencing on TNF- α -treated NPC pyroptosis. **A-B**: miR-155-3p expression in cells was detected using RT-qPCR. **C**: Cell viability was assessed using MTT assay. **D**: IL-1 β and IL-18 levels were detected using ELISA. **E**: NLRP3, GSDMD-N, and cleaved-Caspase1 expressions in cells were detected using western blot. The cell experiments were repeated 3 times independently. The data are expressed as mean \pm standard deviation. The data in panel **A** were analyzed by t test. The data in panels **B-D** were analyzed by one-way ANOVA, and the data in panel **E** were analyzed by two-way ANOVA, followed by Tukey's multiple comparisons test. ** $P < 0.01$

Fig. 5A-B, E). Overexpression of METTL14 resulted in a significant decrease in cell viability ($P < 0.01$, Fig. 5C) and an increase in pyroptosis ($P < 0.01$, Fig. 5D-E), implying that overexpression of METTL14 alleviates the inhibitory effect of ZFAS1 silencing on TNF- α -treated NPC pyroptosis.

Discussion

Due to the functionality of NPCs in maintaining the mechanical and biochemical homeostasis of IVD, loss of NPCs is considered a vital pathological change in IDD [2]. Growing evidence has revealed the crucial role of lncRNAs in the nosogenesis of IDD [1]. This study elucidates that lncRNA ZFAS1 facilitates NLRP3/Caspase-1-mediated NPC pyroptosis in IDD via miR-155-3p/METTL14.

Increasing evidence has emphasized the contribution of NPC pyroptosis to the pathological progression of IDD [7]. Pyroptosis-related proteins, such as NLRP3, Caspase-1, and GSDMD-N, are notably increased in NPCs of IDD patients and murine IDD models [31]. lncRNA ZFAS1 expression has been demonstrated to be positively correlated with TNF- α , IL-1 β , and IL-6 expressions but reversely correlated with IL-10 expression in lumbar disc tissues from patients with lumbar disc degeneration [11]. ZFAS1 knockdown represses IL-1 β -induced NPC apoptosis and ECM degradation [10]. In this study, we isolated and cultured NPCs in vitro, and induced them with different concentrations of TNF- α . We found that as the concentration of TNF- α increased, the cell viability gradually abated and pyroptosis enhanced, accompanied by elevated ZFAS1 expression. After transfecting siRNA

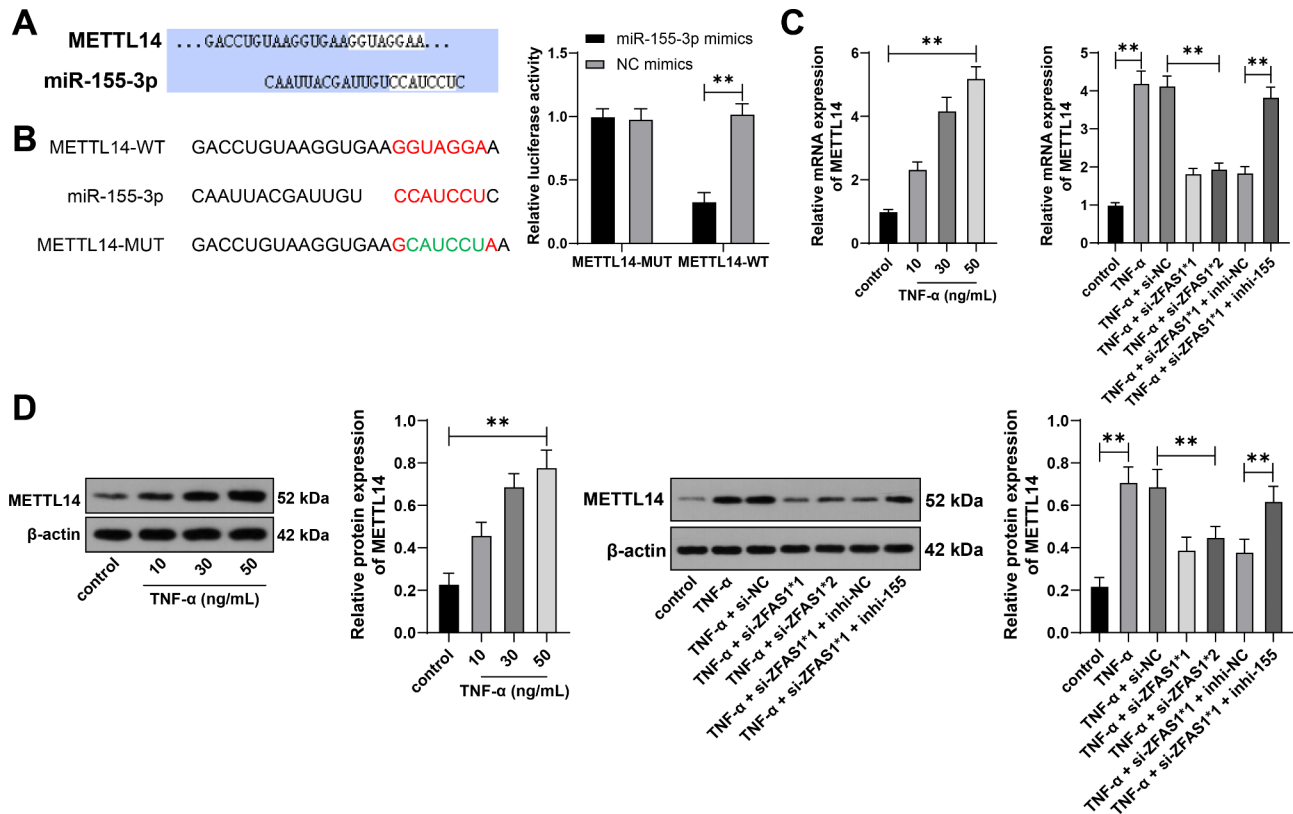


Fig. 4 ZFAS1 promotes METTL14 expression via the ceRNA mechanism. **A:** The binding relationship between miR-155-3p and METTL14 was predicted through the Targetscan database. **B:** The target binding between METTL14 and miR-155-3p was verified using dual-luciferase assay. **C-D:** METTL14 expression in cells were detected using RT-qPCR and western blot. The cell experiments were repeated 3 times independently. The data are expressed as mean \pm standard deviation. The data in panels **C-D** were analyzed by one-way ANOVA, and the data in panel **B** were analyzed by two-way ANOVA, followed by Tukey's multiple comparisons test. $**P < 0.01$

to reduce the expression of ZFAS1 in cells, the expressions of pyroptosis-related proteins (NLRP3, GSDMD-N, and cleaved-Caspase1) were notably diminished, and the levels of pyroptosis-related factors (IL-1 β and IL-18) were also reduced. Collectively, these results revealed that ZFAS1 was highly expressed in TNF- α -treated NPCs and facilitates pyroptosis.

LncRNAs coordinate a wide range of cellular signaling pathways in NPCs by acting as a miRNA sponge, thus modulating various cellular life activities underlying IDD [3]. As an important sponge, ZFAS1 competitively binds to multiple miRNAs. For example, knockdown of ZFAS1 curbs the proliferation and inflammation of fibroblast-like synoviocytes in rheumatoid arthritis via the miR-2682-5p/ADAMTS9 axis [32]. Our experimental results confirmed that ZFAS1 was mainly located in the cytoplasm, suggesting that ZFAS1 might mediate the expression of downstream genes through the ceRNA mechanism. We predicted the binding relationship between ZFAS1 and miR-155-3p through the RNA22 website, and subsequent experimental results also validated that ZFAS1 targeted miR-155-3p expression. Dysregulation of miR-155 accelerates Fas-mediated NPC

apoptosis by repressing FADD and caspase-3 expressions, suggesting the aetiological and therapeutic implication of miR-155 in IDD [33]. miR-155 deficiency contributes to the upregulation of MMP-16 in vivo, which further degrades aggrecan and collagen II, resulting in disc dehydration and degeneration [22]. miR-155-3p is a mature strand grown from miR-155. Upregulation of miR-155-3p expedites the proliferation but depresses the apoptosis of NPCs in IDD by suppressing HIF1 α expression [21]. Similarly, our functional rescue experiments demonstrated that inhibition of miR-155-3p reversed the inhibitory effect of ZFAS1 silencing on TNF- α -treated NPC pyroptosis.

Furthermore, we predicted the binding relationship between miR-155-3p and METTL14 through the Targetscan database. Dual-luciferase assay verified the binding between METTL14 and miR-155-3p. m6A, the most prevalent form of methylation in mRNA and ncRNA, participates in a spectrum of pathological processes underlying IDD [34]. As a key m6A modification enzyme, METTL14 expression is higher in the degenerated lumbar IVD of mice relative to the controls [34]. Moreover, according to literature reports [10, 11], METTL14

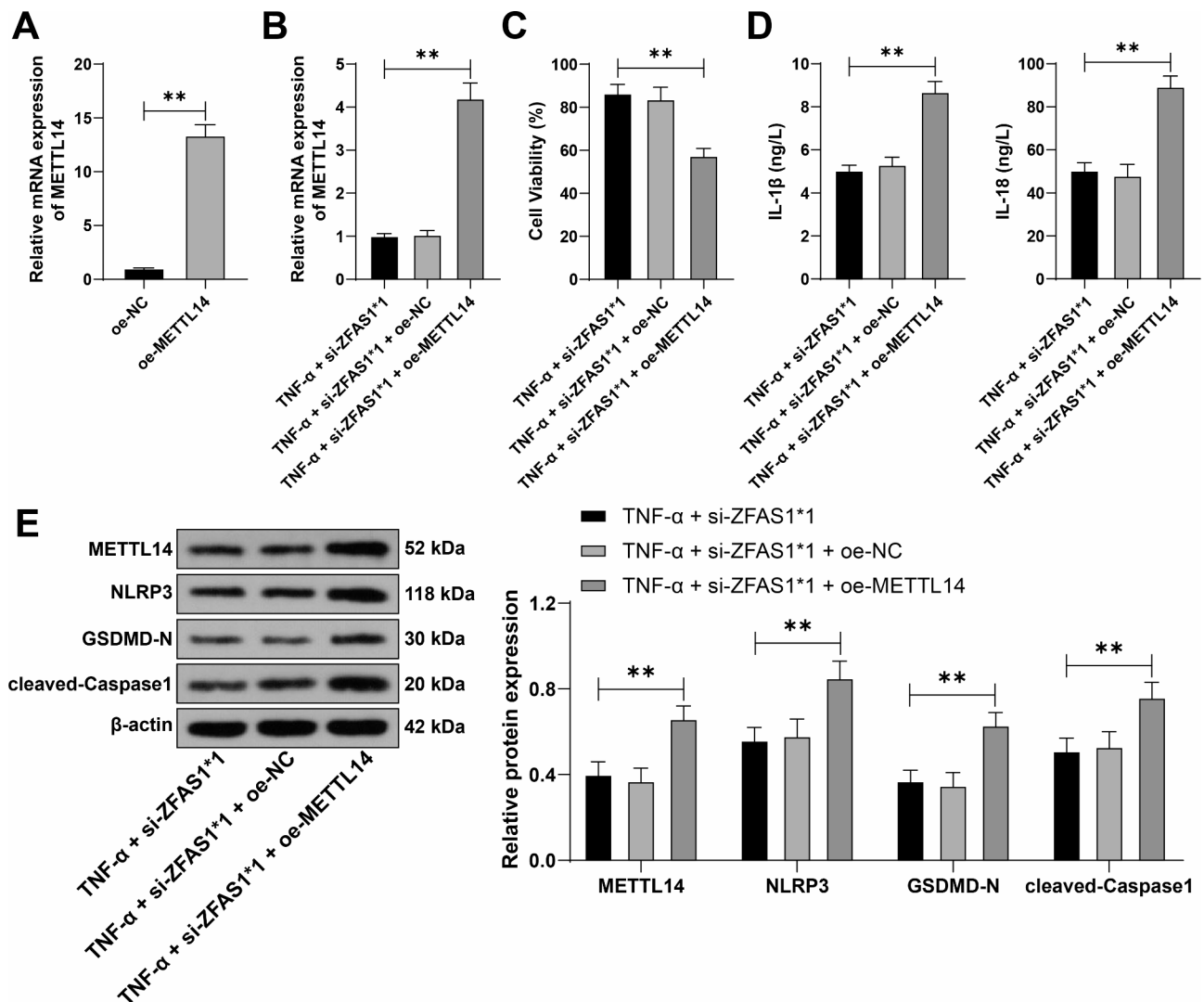


Fig. 5 Overexpression of METTL14 alleviates the inhibitory effect of ZFAS1 silencing on TNF- α -treated NPC pyroptosis. **A-B**: METTL14 expression in cells was detected using RT-qPCR. **C**: Cell viability was assessed using MTT assay. **D**: IL-1 β and IL-18 levels were detected using ELISA. **E**: NLRP3, GSDMD-N, and cleaved-Caspase1 expressions in cells were detected using western blot. The cell experiments were repeated 3 times independently. The data are expressed as mean \pm standard deviation. The data in panel **A** were analyzed by t test. The data in panels **B-D** were analyzed by one-way ANOVA, and the data in panel **E** were analyzed by two-way ANOVA, followed by Tukey's multiple comparisons test. ** $P < 0.01$

expression is increased in human degenerated intervertebral disc tissues, and the higher the grade, the higher the expression. METTL14 is highly present in NP cells from IVD patients, which stabilize NLRP3 mRNA in an IGFBP2-dependent manner and trigger pyroptotic NP cell death [29]. METTL14-mediated m6A modification of DIXDC1 has been reported as a potential therapeutic target to restrain the degeneration of NP in patients with LBP [35]. Our results revealed that METTL14 expression was increased with the increase of TNF- α concentration, decreased with the decrease of ZFAS1 expression, and increased with the decrease of miR-155-3p expression. The above results indicated that ZFAS1 facilitated METTL14 expression by competitively binding to miR-155-3p. METTL14 expression is positively correlated

with m6A level and TNF- α expression in NPCs. Knock-down of METTL14 represses TNF- α -induced cell senescence [30]. METTL14 is abundantly expressed in NPCs from IDD patients and stabilizes NLRP3 mRNA in an IGFBP2-dependent manner. Inhibition of METTL14 improves the viability of NPCs and protects them against pyroptosis [29]. We also found that overexpression of METTL14 alleviates the inhibitory effect of ZFAS1 silencing on TNF- α -treated NPC pyroptosis.

Conclusion

To conclude, ZFAS1 upregulates the transcription level of METTL14 by competitively binding to miR-155-3p, thereby enhancing TNF- α -induced NLRP3/Caspase-1-mediated NPC pyroptosis in IDD. This study also has

certain limitations. Considering that our study is a preliminary exploration, we have only validated our mechanism at the cellular level and what we have revealed is a single mechanism. Whether ZFAS1 regulates apoptosis, autophagy, ferroptosis, and other processes in IDD remains unknown. As a long ncRNA, ZFAS1 still has many downstream miRNAs worthy of exploration. In addition, as an m6A methyltransferase, the downstream mechanism of METTL14 deserves further investigation. In the future, we will further explore the regulation of ZFAS1 on apoptosis, autophagy, and ferroptosis of NPCs in IDD. If conditions permit, we will include clinical samples and further explore the downstream mechanisms of METTL14, thus providing new theoretical knowledge for the treatment of IDD.

Abbreviations

IDD	Intervertebral disc degeneration
LBP	Low back pain
IVD	Intervertebral disc
NPCs	Nucleus pulposus cells
ECM	Extracellular matrix
LncRNAs	Long non-coding RNAs
ZFAS1	Zinc finger antisense 1
miRNAs	MicroRNAs
ceRNAs	Competing endogenous RNAs
METTL14	Methyltransferase-like 14
TNF- α	Tumor necrosis factor- α
PBS	Phosphate-buffered saline
MTT	3-(4,5-dimethylthiazol-2-yl)-2,5-diphenyltetrazolium bromide
ELISA	Enzyme-linked immunosorbent assay
CER	Cytosol extraction reagent
NER	Nuclear extraction reagent
GAPDH	Glyceraldehyde-3-phosphate dehydrogenase
siRNA	Small interfering RNA
RT-qPCR	Real-time reverse transcriptase-polymerase chain reaction
GAPDH	Glyceraldehyde-3-phosphate dehydrogenase
ANOVA	Analysis of variance

Acknowledgements

None declared.

Author contributions

Yuchun Fu: Conceptualization, Data curation, Investigation, Methodology, Visualization, Writing-original draft, Writing-review & editing; Lilei Zhu: Conceptualization, Data curation, Methodology, Validation; Bingxu Ma: Data curation, Formal analysis, Supervision.

Funding

None.

Data availability

No datasets were generated or analysed during the current study.

Declarations

Ethics approval and consent to participate

All animal experiment schemes were approved by the Animal Ethics Committee of Bengbu Medical University and implemented based on the *Guide for the Care and Use of Laboratory Animals* [23].

Consent for publication

Not applicable.

Competing interests

The authors declare no competing interests.

Received: 24 October 2024 / Accepted: 7 January 2025

Published online: 25 February 2025

References

1. Jiang J, Sun Y, Xu G, Wang H, Wang L. The role of miRNA, lncRNA and circRNA in the development of intervertebral disk degeneration (review). *Exp Ther Med*. 2021;21(6):555.
2. Ohnishi T, Iwasaki N, Sudo H. Causes of and molecular targets for the Treatment of Intervertebral Disc Degeneration: a review. *Cells*. 2022;11(3):394.
3. Ran R, Liao HY, Wang ZQ, Gong CY, Zhou KS, Zhang HH. Mechanisms and functions of long noncoding RNAs in intervertebral disc degeneration. *Pathol Res Pract*. 2022;235:153959.
4. Smith LJ, Nerurkar NL, Choi KS, Harfe BD, Elliott DM. Degeneration and regeneration of the intervertebral disc: lessons from development. *Dis Model Mech*. 2011;4(1):31–41.
5. Lyu FJ, Cui H, Pan H, Mc Cheung K, Cao X, Iatridis JC, et al. Painful intervertebral disc degeneration and inflammation: from laboratory evidence to clinical interventions. *Bone Res*. 2021;9(1):7.
6. Zhou KS, Ran R, Gong CY, Zhang SB, Ma CW, Lv JY, et al. Roles of pyroptosis in intervertebral disc degeneration. *Pathol Res Pract*. 2023;248:154685.
7. Ge Y, Chen Y, Guo C, Luo H, Fu F, Ji W, et al. Pyroptosis and intervertebral disc degeneration: mechanistic insights and therapeutic implications. *J Inflamm Res*. 2022;15:5857–71.
8. Jiang C, Chen Z, Wang X, Zhang Y, Guo X, Xu Z, et al. The potential mechanisms and application prospects of non-coding RNAs in intervertebral disc degeneration. *Front Endocrinol (Lausanne)*. 2022;13:1081185.
9. Guo C, Chen Y, Wang Y, Hao Y. Regulatory roles of noncoding RNAs in intervertebral disc degeneration as potential therapeutic targets (review). *Exp Ther Med*. 2023;25(1):44.
10. Wang Z, Liu B, Ma X, Wang Y, Han W, Xiang L. lncRNA ZFAS1 promotes intervertebral disc degeneration by upregulating AAK1. *Open Med (Wars)*. 2022;17(1):1973–86.
11. Deng RY, Hong T, Li CY, Shi CL, Liu C, Jiang FY, et al. Long non-coding RNA zinc finger antisense 1 expression associates with increased disease risk, elevated disease severity and higher inflammatory cytokines levels in patients with lumbar disc degeneration. *Med (Baltim)*. 2019;98(52):e18465.
12. Zhu J, Zhang X, Gao W, Hu H, Wang X, Hao D. lncRNA/circRNA-miRNA-mRNA ceRNA network in lumbar intervertebral disc degeneration. *Mol Med Rep*. 2019;20(4):3160–74.
13. Wang C, Cui L, Gu Q, Guo S, Zhu B, Liu X, et al. The mechanism and function of miRNA in intervertebral disc degeneration. *Orthop Surg*. 2022;14(3):463–71.
14. Oliviero A, Della Porta G, Peretti GM, Maffulli N. MicroRNA in osteoarthritis: physiopathology, diagnosis and therapeutic challenge. *Br Med Bull*. 2019;130(1):137–47.
15. Giordano L, Porta GD, Peretti GM, Maffulli N. Therapeutic potential of microRNA in tendon injuries. *Br Med Bull*. 2020;133(1):79–94.
16. Gargano G, Oliviero A, Oliva F, Maffulli N. Small interfering RNAs in tendon homeostasis. *Br Med Bull*. 2021;138(1):58–67.
17. Gargano G, Oliva F, Oliviero A, Maffulli N. Small interfering RNAs in the management of human rheumatoid arthritis. *Br Med Bull*. 2022;142(1):34–43.
18. Gargano G, Asparago G, Spiezia F, Oliva F, Maffulli N. Small interfering RNAs in the management of human osteoporosis. *Br Med Bull*. 2023;148(1):58–69.
19. Cazzanelli P, Wuertz-Kozak K. MicroRNAs in intervertebral disc degeneration, apoptosis, inflammation, and mechanobiology. *Int J Mol Sci*. 2020;21(10):3601.
20. Zheng J, Zeng P, Zhang H, Zhou Y, Liao J, Zhu W, et al. Long noncoding RNA ZFAS1 silencing alleviates rheumatoid arthritis via blocking mir-296-5p-mediated down-regulation of MMP-15. *Int Immunopharmacol*. 2021;90:107061.
21. Zhou X, Li J, Teng J, Liu Y, Zhang D, Liu L, et al. microRNA-155-3p attenuates intervertebral disc degeneration via inhibition of KDM3A and HIF1 α . *Inflamm Res*. 2021;70(3):297–308.
22. Zhang WL, Chen YF, Meng HZ, Du JJ, Luan GN, Wang HQ, et al. Role of miR-155 in the regulation of MMP-16 expression in intervertebral disc degeneration. *J Orthop Res*. 2017;35(6):1323–34.
23. Jones-Bolin S. Guidelines for the care and use of laboratory animals in biomedical research. *Curr Protoc Pharmacol*. 2012;Appendix 4:Appendix 4B.
24. Jiang Y, Xie Z, Yu J, Fu L. Resveratrol inhibits IL-1 β -mediated nucleus pulposus cell apoptosis through regulating the PI3K/Akt pathway. *Biosci Rep*. 2019;39(3):BSR20190043.

25. Mas-Ponte D, Carlevaro-Fita J, Palumbo E, Hermoso Pulido T, Guigo R, Johnson R. LncAtlas database for subcellular localization of long noncoding RNAs. *RNA*. 2017;23(7):1080–7.
26. Loher P, Rigoutsos I. Interactive exploration of RNA22 microRNA target predictions. *Bioinformatics*. 2012;28(24):3322–3.
27. Agarwal V, Bell GW, Nam JW, Bartel DP. Predicting effective microRNA target sites in mammalian mRNAs. *Elife*. 2015;4:e05005.
28. Livak KJ, Schmittgen TD. Analysis of relative gene expression data using real-time quantitative PCR and the 2⁻(Delta Delta C(T)) method. *Methods*. 2001;25(4):402–8.
29. Yuan X, Li T, Shi L, Miao J, Guo Y, Chen Y. Human umbilical cord mesenchymal stem cells deliver exogenous miR-26a-5p via exosomes to inhibit nucleus pulposus cell pyroptosis through METTL14/NLRP3. *Mol Med*. 2021;27(1):91.
30. Zhu H, Sun B, Zhu L, Zou G, Shen Q. N6-Methyladenosine Induced miR-34a-5p promotes TNF-alpha-Induced Nucleus Pulposus Cell Senescence by Targeting SIRT1. *Front Cell Dev Biol*. 2021;9:642437.
31. Wang Z, Li X, Yu P, Zhu Y, Dai F, Ma Z, et al. Role of Autophagy and Pyroptosis in intervertebral disc degeneration. *J Inflamm Res*. 2024;17:91–100.
32. Yang S, Yin W, Ding Y, Liu F. Lnc. RNA ZFAS1 regulates the proliferation, apoptosis, inflammatory response and autophagy of fibroblast-like synoviocytes via miR-2682-5p/ADAMTS9 axis in rheumatoid arthritis. *Biosci Rep*. 2020;40(8):BSR20201273.
33. Wang HQ, Yu XD, Liu ZH, Cheng X, Samartzis D, Jia LT, et al. Dereglated miR-155 promotes Fas-mediated apoptosis in human intervertebral disc degeneration by targeting FADD and caspase-3. *J Pathol*. 2011;225(2):232–42.
34. Zhu B, Chen HX, Li S, Tan JH, Xie Y, Zou MX, et al. Comprehensive analysis of N6-methyladenosine (m(6)A) modification during the degeneration of lumbar intervertebral disc in mice. *J Orthop Translat*. 2021;31:126–38.
35. Tu J, Li W, Hansbro PM, Yan Q, Bai X, Donovan C, et al. Smoking and tetramer tryptase accelerate intervertebral disc degeneration by inducing METTL14-mediated DIXDC1 m(6) modification. *Mol Ther*. 2023;31(8):2524–42.

Publisher's note

Springer Nature remains neutral with regard to jurisdictional claims in published maps and institutional affiliations.